AIP | Journal of Applied Physics

Degradation mechanism beyond device self-heating in high power light-emitting diodes

K. C. Yung, H. Liem, H. S. Choy, and W. K. Lun

Citation: J. Appl. Phys. **109**, 094509 (2011); doi: 10.1063/1.3580264
View online: http://dx.doi.org/10.1063/1.3580264
View Table of Contents: http://jap.aip.org/resource/1/JAPIAU/v109/i9
Published by the American Institute of Physics.

Related Articles

Temperature-dependence of the internal efficiency droop in GaN-based diodes
Appl. Phys. Lett. 99, 181127 (2011)

Localized surface plasmon-enhanced electroluminescence from ZnO-based heterojunction light-emitting diodes
Appl. Phys. Lett. 99, 181116 (2011)

Performance enhancement of blue light-emitting diodes with AlGaN barriers and a special designed electron-blocking layer
J. Appl. Phys. 110, 093104 (2011)

A light emitting diode based photoelectrochemical screener for distributed combinatorial materials discovery
Rev. Sci. Instrum. 82, 114101 (2011)

Promotion of hole injection enabled by GaInN/GaN light-emitting triodes and its effect on the efficiency droop
Appl. Phys. Lett. 99, 181115 (2011)

Additional information on J. Appl. Phys.

Journal Homepage: http://jap.aip.org/
Journal Information: http://jap.aip.org/about/about_the_journal
Top downloads: http://jap.aip.org/features/most_downloaded
Information for Authors: http://jap.aip.org/authors

ADVERTISEMENT

Submit Now

Explore AIP's new open-access journal

• Article-level metrics now available

• Join the conversation! Rate & comment on articles

Downloaded 08 Nov 2011 to 158.132.161.9. Redistribution subject to AIP license or copyright; see http://jap.aip.org/about/rights_and_permissions

JOURNAL OF APPLIED PHYSICS **109**, 094509 (2011)

Degradation mechanism beyond device self-heating in high power light-emitting diodes

K. C. Yung,[a)] H. Liem, H. S. Choy, and W. K. Lun
Department of Industrial and Systems Engineering, Hong Kong Polytechnic University, Hung Hom, Kowloon 233, Hong Kong

(Received 9 February 2011; accepted 13 March 2011; published online 12 May 2011)

A unique degradation property of high power InGaN/GaN multiple quantum well (MQW) white light-emitting diodes (LEDs) was identified. The LEDs were stressed under different forward-currents. The various ageing characteristics were analyzed for both the electrical response and electro-luminescence (*EL*) spectra. The Raman spectroscopy allowed noninvasive probing of LED junction temperature profiles which correlated well with the *EL* characteristics, showing a junction temperature drop during degradation at certain current levels. In addition to the common observations: (1) a broadening of the light intensity-current (*L-I*) characteristic in the nonlinear regime, and (2) a shift of the current-voltage (*I-V*) dependence to higher current levels, the *EL* spectra showed different temperature responses of the two blue emission peaks, 440 and 463 nm. The former was temperature sensitive and thus related to shallow defect levels, while the latter was thermally stable and deeper defect states were involved in the degradation process. This unique selection rule resulted in the enhancement of the blue emission peak at 463 nm after degrading the LEDs. This study suggests that LED device heating is not directly linked to the degradation process. © *2011 American Institute of Physics*. [doi:10.1063/1.3580264]

I. INTRODUCTION

In recent years, lighting using white LEDs has become very attractive due to their low power consumption, long operating time, and environmental benefits (no mercury).[1–3] Currently, the prevailing method for fabricating white LEDs is by using a blue GaN-based light-emitting diode (LED) coated with a yellow-emitting phosphor. This simple structure gives LEDs high luminous efficacy ~ 150 lm/W.[4–6] The degradation of light emitting diodes is a multi-faceted problem that involves change of defect population, catastrophic optical destruction, metal diffusion and electrode delamination.[7] It is an elusive subject for research due to the presence of difficulties in identifying a specific degradation mechanism in different types of LEDs. In fact, different causes may dominate even in a single type of diode, and different degradation mechanisms can be observed simultaneously. The origins of the degradation of LEDs submitted to accelerated ageing tests have been intensively investigated.[8–26] It was accepted that a significant reduction in the internal quantum efficiency of the LEDs resulted from a constant current stress. This degradation was characterized by the increase in the nonradiative recombination in the active junction of the LEDs due to the propagation of defects,[13,25,26] or caused by the migration of impurities or dopants in the multiple quantum well (MQW) region. In addition, operating at high temperature, GaN-based LEDs could have their optical properties significantly degraded. This temperature degradation was determined by the deterioration of the electrical properties of the ohmic contact and p-type semiconductor material triggered by the chemical reaction between dopants and hydrogen atoms.[16,20] Besides, the self-heating in LEDs affected the device performance and was generally suggested to be correlated with the device lifetime. Moreover, darkening of the encapsulation and phosphor systems by thermal activation had the immediate effect of altering the colors emitted by the LEDs.[12,13]

Step-stress testing is employed as a way to test the LED's accelerated life. Although there are many varieties of step-stress testing, the type used is the one in which a LED is tested at a given current density (stress level) for a certain amount of time. At the end of that time, if the LED survives, i.e., the electro-luminance spectrum shows the same intensity and features for a specific lower current, the stress level is increased and held for another amount of time. The process is repeated until the LED degrades, i.e., the electro-luminance spectrum shows different features. The degradation or performance data is then directly related to the presumed failure of the LED in question and each electro-luminance spectrum is monitored as a function of current.

The small size of the LED die and its encapsulation makes measuring the diode junction temperature difficult to perform with direct methods, such as thermocouples and infrared cameras. *EL* spectrum is not a good quantitative indicator due to the fact that both the *EL* peak position and intensity are affected by factors other than temperature, such as piezoelectric effect and charge density. Noncontact Raman spectroscopy is employed for measuring the junction temperature of InGaN/GaN LED due to its high spatial resolution and measurement capabilities of devices under electrical bias.[27,28]

In this paper, ageing-induced changes in optical *EL* and electrical *I-V* diode characteristics are considered to be a measure of degradation. Raman temperature measurement is

[a)]Electronic mail: mfkcyung@inet.polyu.edu.hk.

 © 2011 American Institute of Physics

Downloaded 08 Nov 2011 to 158.132.161.9. Redistribution subject to AIP license or copyright; see http://jap.aip.org/about/rights_and_permissions

correlated with the *EL* characteristics. We describe in detail the degradation processes involving the different thermal responses of the three emission peaks with increasing currents. Subsequently, LED degradation modes are highlighted and enhancement of a specific blue emission is found to be related to the selection of defect levels during degradation. We suggest that an LED is degrading when the two blue emissions in the electro-luminance spectrum start showing different temperature sensitivities. Providing some insight into degradation mechanisms beyond simple device heating, a unique characteristic in the degradation of high power InGaN/GaN LEDs by stressed current is identified.

II. EXPERIMENTAL PROCEDURES

The samples examined in the test were commercial high-power blue LEDs from Philips Lumileds K2. They employ a multi-quantum well structure having layers of InGaN/GaN on the sapphire substrate. The LED die has a standard area $\sim 1 \times 1$ mm^2, is mounted on top of a silicon chip using gold stud bumps, which is in turn bounded to the heat-sink slug. The LED die is bonded in a flip-chip way, and encapsulated with an epoxy lens-InGaN/GaN chip structure. The epoxy lens was removed by hot H_2SO_4 in the experiment so that its effect on degradation can be ignored.

The accelerated current test was performed with a forward current equal to or larger than 2100 mA for an hour. The evolution of current-voltage (*I–V*) characteristics and optical output of the LEDs were measured by an HP 4145B semiconductor parameter analyzer and a silicon photo-array spectrometer. A simple test configuration was used to measure the electroluminescence (*EL*) of the LED samples. The average surface temperature of the LEDs under a forward-current was measured using an NEC MRI 9100 thermo tracer.

Unpolarized Raman spectra on the GaN were obtained using a Renishaw 2000 confocal Raman spectrometer. An argon ion laser with 514 nm line was used as the excitation. It was transmitted through the sapphire substrate and focused on the GaN. The spectra were measured in the backscattering geometry at currents from 0 to 2800 mA. An integration time of 10 s was used for each measurement and each raw spectrum was then subject to a curve-fitting routine (Grams 32, Galactic Industries, Salem, US) to obtain the Raman intensities of the 571.1 cm^{-1} at each point.

III. RESULTS AND DISCUSSION

The inset of Fig. 1 shows the SEM image of a Philips LED used in the study. The encapsulating lens was removed, and the vertical conduction wires were shown. Nominal operating current was in the range of 200–2800 mA, and the corresponding current densities were from 20 to 280 A/cm^2 for a 1 mm^2 square chip. Figure 1 shows a typical room temperature Raman spectrum of GaN, showing the E_2^H phonon mode for GaN which is located at 571.1 cm^{-1}. The A_1(LO) mode and the sapphire substrate peaks are observed at 736.2 and 419.4 cm^{-1}, respectively. The E_2^H mode is selected because it is very sensitive to biaxial stress in GaN films.[29] It should be noted that the E_2^H already exhibited a blueshift of

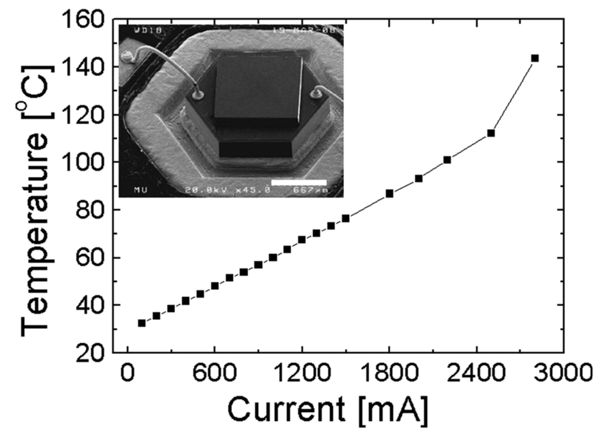

FIG. 1. The room-temperature Raman spectrum measured from an InGaN/GaN LED die. The inset (left) shows the SEM image of the LED die on silicon submount with lens removed (Courtesy of MuAnalysis). The inset (right) shows the calibration curve which returns the junction temperature of an InGaN/GaN LED against the shift of the E_2^H mode.

1.7 cm^{-1} due to the compressive stress existed in the InGaN epilayer.[30] The A_1(LO) phonon is not suitable for determining the junction temperature due to the fact that the coupled mode of A_1(LO) phonons and plasmons is measured in the spectrum instead of the pure A_1(LO) phonon in the doped layers of the *pn* junction. Link *et al*. have reported that the temperature dependences of the E_2^H mode can be described by a model which takes into account the anharmonicity of crystal lattice potential and the thermal (i.e., CTE) mismatch between the sapphire substrate and the layers.[31] However, the strain-induced contribution $\Delta w_s(T)$ to the frequency shift is insignificant when compared to that due to thermal expansion $\Delta w_e(T)$ of the lattice and optical phonon decay $Dw_d(T)$.[31] The phonon frequency can then be related to material temperature by the equation:

$$\omega(T) = \omega_0 - \frac{A}{e^{Bhc\omega_0/kT} - 1} \quad (1)$$

with ω_0, A and B are the Grüneisen parameters and are defined by Hayes *et al*.[32] and h is the Planck constant, c is the speed of light, k is the Boltzmann constant and T is the material temperature. The E_2^H peak shift performed at 0 mA (and thus room temperature) was selected and calibrated. The values of ω_0, A and B are determined to be 272.36, 17.9, and 0.99 cm^{-1}, respectively. The shift $\Delta\omega$ was accurate to 0.05 cm^{-1}, or 1 K. A calibration curve which returns the junction temperature of the InGaN/GaN LED against the shift of the E_2^H mode is derived and plotted in the inset (right) of Fig. 1.

Figure 2 shows the *EL* spectra obtained from the Philips LED at various current levels. There are two main light emissions: the blue emission (440 nm, Royal blue) which is assigned to homogeneous InGaN quantum well (QW) due to the prohibition of extra phase separation by residual strain, and the green one (517 nm) which corresponds to In-rich quantum dots (QDs). In addition to the 440 nm emission, the spectra reveal a second weak peak at lower frequency shifted by 23 nm. This is not the resonance case in Fabry–Perot cavity formed by the large reflectivity at the GaN interfaces.

Downloaded 08 Nov 2011 to 158.132.161.9. Redistribution subject to AIP license or copyright; see http://jap.aip.org/about/rights_and_permissions

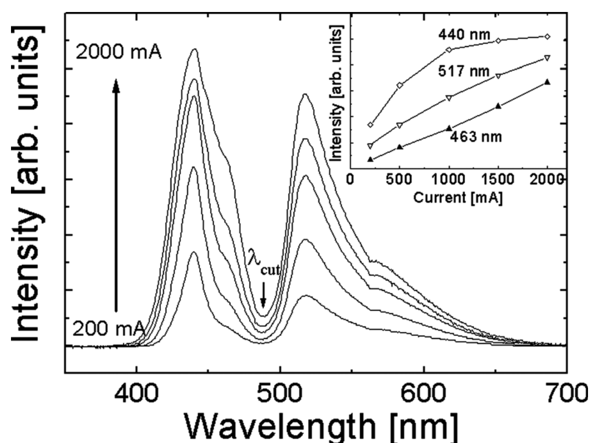

FIG. 2. Normalized electro-luminance (*EL*) spectra from an InGaN/GaN LED for different currents. The inset shows the dependences of the three emissions on current amplitudes.

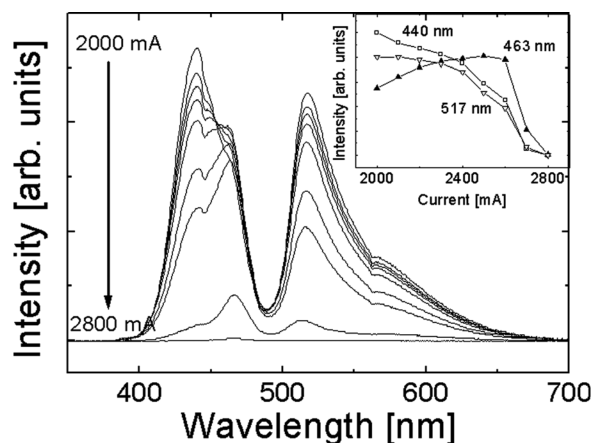

FIG. 3. Normalized electro-luminance (*EL*) spectra from an InGaN/GaN LED submitted to different stress currents. The inset shows the dependences of the three emissions on current amplitudes.

Because the cavity length would be ~1726 nm which is of two order cavity dimension in our case. It is proposed that the inhomogeneous InGaN part contributes to the relatively weak 463 nm emission. The bipartition of the spectrum was measured at a wavelength value $\lambda_{cut} = 488$ nm. These two peaks increase as the injection current increases. The inset of Fig. 2 shows the dependences of the intensity of *EL* emissions on the current densities. It indicates that the intensity of the blue emission (440 nm) increases more initially than that of green one due to the larger emission area. At high currents, this emission is saturated while the band at 463 nm is not. Similar intensity changes at various currents have been observed in hybrid GaN-PTA LEDs.[33] The intensity of the green emission (517 nm) is nearly linear to the injection current. The difference in intensity between the two emissions increases with the injection level, but decreases under a large injection current (1000 mA). At the later stage, the decrease in intensity difference results from the joule heating at a high injection current which weakens the quantum confinement in QW. The effect of joule heating on excitons in QDs is not significant (only a small decrease in intensity difference) due to their large confinement energy. The saturation of the blue emission, however, is essentially the result of low quantum efficiency at high junction temperatures.

It is suggested that the blue emission from QW blue shifts as the current increases.[34] This is due to the filling of localized states in the In-rich region, and to the screening of the piezoelectric field in strained MQW structures.[35,36] There is no wavelength shift in either emission at low injection current. This may be complemented by the red-shift factor or the charge transfer modified piezoelectric field.[37] Under high injection current, high junction temperature may cause redshift to occur in the peak emissions.[38] There are no wavelength shifts, suggesting that the emissions are less influenced by junction temperature. The two emissions (440 and 465 nm) are not found exclusively on Philips LEDs, they are found also on LEDs made by other manufacturers, for example Cree XLamp, Samsung Sunnix, and Wai Chi Elect, and other research groups using InGaN-based LEDs that adopt a similar white light emission method.[33,34,37,38] However, we observed insignificant blue or red shifts (< 0.5 cm^{-1}) in wavelengths for both the emissions which may be understood as compensation between band-filling, screening, and piezoelectric field-induced quantum confined Stark effects (QCSE).[39] This is the reason why we chose Philips LEDs for studying the degradation mechanism. The spectrum is reversible when the current is below 2100 mA, i.e., same features and intensities of the different emission bands are reserved for a specific current.

The relative intensity–current characteristic of an LED after ageing is shown in the inset of Fig. 3. The amplitudes of the main *EL* which peak at 440 and 517 nm, decrease as the current increases as shown in the inset of Fig. 3. However, the amplitude of the blue emission at 463 nm does not decrease but *increases* gradually to a maximum at 2500 mA which is 47% more than the initial value shown in the inset. This intensity enhancement or the late degradation has not been highlighted before even though similar *EL* features have been observed in In-doped GaN and N-doped GaP LEDs.[9,19,40] In Fig. 4, the Raman shift of the E_2^H mode and the LED junction temperature deduced there from are plotted in dependence on the applied current. At zero current, the phonon wave number equals 571.1 cm^{-1} which corresponds to the room temperature of nearly 300K. The phonon

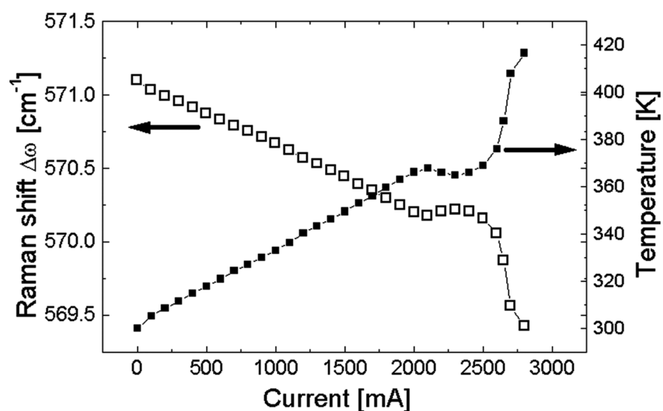

FIG. 4. Raman shift of the E_2^H phonon (left y-axis) and the LED junction temperature deduced there from (right y-axis).

Downloaded 08 Nov 2011 to 158.132.161.9. Redistribution subject to AIP license or copyright; see http://jap.aip.org/about/rights_and_permissions

frequency starts to decrease at 100 mA and shifts downwards to 570.2 cm^{-1} at 2100 mA. This corresponds to an increase of the temperature from 300 to 368K. At 2100 mA, it starts to decrease and equals 365K at 2300 mA. The intensity enhancement in *EL* is accompanied by a decrease in temperature. The phonon frequency starts to decrease again when the current is above 2300 mA. Due to the charge competition between the three emissions, the temperature decreases to 365K at 2300 mA but not 2500 mA. It is worth mentioning that such temperature profile cannot be observed using thermocouples nor infrared cameras as the surrounding device components and optics may average out the difference while only surface temperature can be measured.

The different variations in the two emission peaks with increasing current may be explained as follows. It is postulated that the 440 nm peak is essentially related to shallow defect energy level which is not thermally stable for electrons at this level.[41] However, by taking a transition to the conduction band, most electrons in the shallow level are thermally ionized as the temperature increases to above 368 K (at 2100 mA), and may recombine nonradiatively. This results in a rapid decrease in the luminescence intensity at 440 nm. Joule heating increases which could cause an elevation of junction temperature. However, Raman temperature measurement shows that the temperature decreases initially and increases when the current is above 2300 mA. It is then postulated that the emission peak of 463 nm exhibits a smaller dependence on the temperature, suggesting that most of the electrons that are excited in the deeper defect energy levels, are thermally stable.[41] The electrons may return to the ground state via radiative transitions at current above 2100 mA, results in decreasing temperature. The intensity enhancement with increasing current may thus be mainly induced by enhanced radiative recombination. At current above 2300 mA, joule heating keeps increasing and junction temperature increases. Moe *et al*. reported that AlGaN-based LED heating, was correlated with the initial drop in output power during burn-in, but is not directly linked to the total degradation over the lifetime of the device.[42] Their observation is not the same as ours because their LEDs are aged thermally at the equivalent temperatures, such that they have less degradation that those electrically biased. The degradation under operating currents is attributed to the increased nitrogen vacancy formation caused by energetic electrons at the junction.

The current-voltage (*I-V*) characteristics of an LED before and after forward-current stress are shown in Fig. 5. Compared to the curve before ageing, the stressed curve shows a significant current increase in the low forward bias voltage V_f. Three characteristic regions of LED operation can be observed: (1) Low bias region where $V_f < 2.6$ V, the *I–V* characteristic is dominated by the nonradiative recombination of carriers in the space charge region ($I < 1.8$ mA). (2) As the bias voltage is increased such that $V_f > 2.6$ V, the injected carriers occupy the active layer and thus radiative recombinations become dominant. (3) With the bias voltages increasing, $V_f > 3.0$ V, the *I–V* characteristic, which is essentially ohmic, results from the device's series resistance. At the same low forward bias voltage, the ageing effect is to

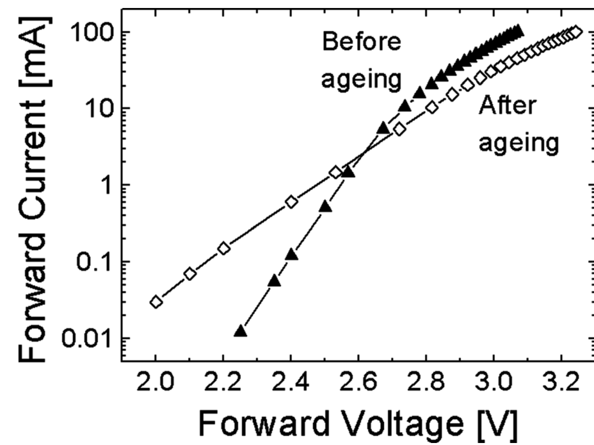

FIG. 5. *I-V* characteristics of the LEDs before and after forward-current stress.

shift the *I–V* curve to a higher current. This change takes place only in the higher forward bias region when the LED starts to radiate (2.6–3.0 V). The diode ideality factor is increased (~2.8) in the low bias region too, but is decreased in the high bias range (~4.0) due to the ageing effects. However, as pointed out by Masui *et al.* that the measured ideality factors are higher via *I-V* method when quantum well structure takes over the role of the recombination plane.[43] Obtained ideality factors on commercial LEDs could be corrected by a factor of 2 via photoluminescence technique. These values are 1.4 and 2.0 in the low and high bias ranges, respectively, which agree well with the Sah-Noyce-Shockley (SNS) analysis.[44] We do not consider reverse-bias stress, as the physical model for defect creation could be different, as it involves the creation of deep-level states in the cladding layers and results in avalanche breakdown.

The shifting of the *I–V* curve is an indication of defect generation in the active layer. The nonradiative recombination rates and thus the current are enhanced by the new defects in the active layer.[45] This excess current component is also visible in the high-voltage range even if the radiative recombination is dominating over the nonradiative one. A large amount of heat is generated in the active layer where the majority of carriers recombine at a high-current density. This results in a high junction temperature. Hot carriers can transfer enough energy to the lattice displacing the atoms and breaking the metal–N bonds.[45] The presence of defect density due to ageing is observed as being more pronounced in the low bias *I–V* characteristic of LED.

The Luminance-Current (*L–I*) characteristics before and after ageing are shown in Fig. 6. The *L–I* curve is traditionally divided into a nonlinear and a linear region.[46–48] The linear region is a result of the radiative recombination dominating in the active layer at a high bias voltage. In the nonlinear portion, the radiative intensity increases in roughly a quadratic manner as the forward bias current increases. The nonlinear region is not considered here as radiative emissions and their relationship with defect generations due to degradation are the main concern in this study.

The *L–I* curve is almost linear above 3 mA before ageing, whereas it became linear at slightly higher values above

Downloaded 08 Nov 2011 to 158.132.161.9. Redistribution subject to AIP license or copyright; see http://jap.aip.org/about/rights_and_permissions

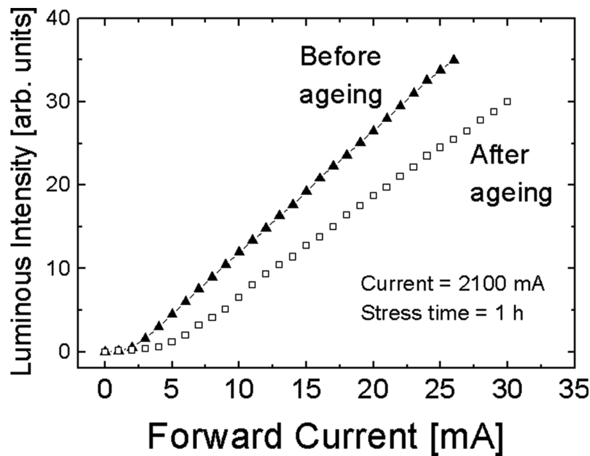

FIG. 6. *L-I* characteristics of the LEDs before and after ageing. A current of 2100 mA was used.

6 mA after ageing. This behavior can be understood by using the continuity equation for the injected electrons n:[49]

$$\frac{dn}{dt} = \frac{J}{ed} - An - Bn^2. \tag{2}$$

The change in current is equal to the current injection rate, J/ed, minus the nonradiative rate, An, and radiative emission rate, Bn^2. Here J is the current density, e the electron charge, d the thickness of the active layer, and A and B are the nonradiative and radiative recombination coefficients, respectively. Due to the large bandgap energy of InGaN, Auger recombination is neglected. Assuming also background carrier density is negligible, thus electron and hole are of equal concentration. As the current density increases the radiative recombination of carriers, the Bn^2 term starts to dominate such that the light output L becomes linear with current density J until the current induced heating results in a sublinear increase of L with J. At steady-state conditions $dn/dt = 0$, the light emission is then

$$L = Bn^2 \approx \frac{J}{ed}. \tag{3}$$

The nonradiative recombination coefficient A can be expressed by the Shockley-Hall-Read recombination rate:[50]

$$A = N_t v_{th} \sigma \tag{4}$$

Where N_t is the defect density of trap, v_{th} the thermal velocity, and σ the electron capture cross section. It is assumed that the capture cross sections and the thermal velocity are equal for both electrons and holes. An increase in defect density N_t, will then reduce the total light intensity L for a specific forward current. It is worth mentioning that the total light intensity L defined here refers to the summation of the three intensities, $L_{440\text{nm}}$, $L_{463\text{nm}}$, and $L_{517\text{nm}}$ shown in the inset of Fig. 2. Similarly, the same summation is applied to the reduction in light intensity shown in the inset of Fig. 3. An increase in defect density N_t, will cause the light intensity L to decrease for a fixed current. Due to the ageing treatment, the defect density N_t is increased roughly by a factor of 1.3, as shown in Fig. 5. In the active layer the generation of defects during the ageing treatment reduces the light emission from the LED in the low current regime. However, these nonradiative recombination processes become saturated at high current levels.

IV. CONCLUSION

In summary, we have presented methods of identifying the degradation mechanism of InGaN/GaN blue LEDs using the current-voltage and electro-luminance characteristics. Interpretation of the change in *I-V* curves in a high-current regime is a manifestation of defect generation in the LED's active layer. The defect generation can be identified by the *L-I* characteristic that the nonlinear part of the curve shifts to higher current levels. The 440 nm blue emission from the homogeneous InGaN quantum well (QW) was temperature sensitive and thus related to shallow defect levels, while the 463 nm emission from inhomogeneous QW was thermally stable and intensity enhancement was observed. Raman spectroscopy was used to determine the junction temperature at various operating currents. A new degradation characteristic of high power GaN-based white LEDs was identified. Furthermore, the local temperature of InGaN/GaN LED in dependence on the applied current was determined, demonstrating the potential of our results for the investigation of optoelectronic devices in operation. Experiments on investigating the nonradiative defect centers generation mechanism in the active layers are underway and will be reported later.

ACKNOWLEDGMENTS

This work was funded by the Hong Kong Innovation Technology Fund (ITF) under project number ITS/257/09FP.

[1]M. G. Craford, Proc. SPIE **4776**, 1 (2002).
[2]J. K. Park, C. H. Kim, S. H. Park, H. D. Park, and S.Y. Choi, Appl. Phys. Lett. **84**, 1647 (2004).
[3]H. S. Jang, W.B. Im, D.C. Lee, D.Y. Jeon, and S. S. Kim, J. Lumin. **126**, 371 (2007).
[4]A. A. Efremov, N. I. Bochkareva, R. I. Gorbunov, D. A. Larinovich, Y. T. Rebane, D. V. Tarkhin, and Y. G. Shreter, Semiconductors **40**, 605 (2006).
[5]Smart Lighting: New LED Drops The "Droop," available at http://www.sciencedaily.com/releases/2009/01/090113123718.htm.
[6]R. Stevenson, *IEEE Spectrum*, August 2009, available at http://www.spectrum.ieee.org/semiconductors/optoelectronics/the-leds-dark-secret.
[7]S. O'Hara, J. Phys. D: Appl. Phys. **10**, 409 (1977).
[8]X. A. Cao, P. M. Sandvik, S. M. LeBoeuf, and S. D. Arthur, Microelectron. Reliab. **43**, 1987 (2003).
[9]Z. Z. Chen, J. Zhao, Z. X. Qin, X. D. Hu, T. J. Yu, Y. Z. Tong, Z. J. Yang, X. Y. Zhou, G. Q. Yao, B. Zhang, and G. Y. Zhang, Phys. Status Solidi B **241**, 2664 (2004).
[10]N. Narendran, Y. Gu, J. P. Freyssinier, Y. Yu, and L. Deng, J. Cryst. Growth **268**, 449 (2004).
[11]S. Levada, M. Meneghini, G. Meneghesso, and E. Zanoni, IEEE Trans. Device Mater. Reliab. **5**, 688 (2005).
[12]M. Meneghini, L. Trevisanello, S. Podda, S. Buso, G. Spiazzi, G. Meneghesso, and E. Zanoni, Proc. SPIE **6337**, 63370R (2006).
[13]F. Rossi, M. Pavesi, M. Meneghini, G. Salviati, M. Manfredi, G. Meneghesso, A. Castaldini, A. Cavallini, L. Rigutti, U. Strass, U. Zehnder, and E. Zanoni, J. Appl. Phys. **99**, 053104 (2006).
[14]L. Trevisanello, M. Meneghini, G. Mura, M. Vanzi, M. Pavesi, G. Meneghesso, and E. Zanoni, IEEE Trans. Device Mater. Reliab. **8**, 304 (2008).

Downloaded 08 Nov 2011 to 158.132.161.9. Redistribution subject to AIP license or copyright; see http://jap.aip.org/about/rights_and_permissions

[15]T. Yu, S. Shang, Z. Chen, Z. Qin, L. Lin, Y. Yang, and G. Zhang, J. Lumin. **122–123**, 696 (2007).
[16]M. Meneghini, L.-R. Trevisanello, U. Zehnder, G. Meneghesso, and E. Zanoni, IEEE Trans. Electron Devices **54**, 3245 (2007).
[17]S. Buso, G. Spiazzi, M. Meneghini, and G. Meneghesso, IEEE Trans. Device Mater. Reliab. **8**, 312 (2008).
[18]S. N. Lee, H. S. Paek, J. K. Son, H. Kim, K. K. Kim, K. H. Ha, O. H. Nam, and Y. Park, J. Electroceram. **23**, 406 (2009).
[19]J. Hu, L. Yang, and M. W. Shin, J. Phys. D: Appl. Phys. **41**, 035107 (2008).
[20]M. Meneghini, L. Rigutti, L. Trevisanello, A. Cavallini, G. Meneghesso, and E. Zanoni, J. Appl. Phys. **103**, 063703 (2008).
[21]L. Trevisanello, F. De Zuani, M. Meneghini, N. Trivellin, E. Zanoni, and G. Meneghesso, IEEE International Reliability Physics Symposium IRPS 2009, Montreal, 26–30 April 2009.
[22]M. Meneghini, U. Zehnder, B. Hahn, G. Meneghesso, and E. Zanoni, IEEE Electron Device Lett. **30**, 1051 (2009).
[23]S. K. Jeon, J. G. Lee, E. H. Park, J. H. Jang, J. G. Lim, S. K. Kim, and J. S. Park, Appl. Phys. Lett. **94**, 131106 (2009).
[24]L. Rigutti, L. Basirico, A. Cavallini, M. Meneghini, G. Meneghesso, and E. Zanoni, Semicond. Sci. Technol. **24**, 055015 (2009).
[25]A. Y. Polyakov, N. B. Smirnov, A. V. Govorkov, J. Kim, B. Luo, R. Mehandru, F. Ren, K. P. Lee, S. J. Pearton, A. V. Osinsky, and P. E. Norris, J. Appl. Phys. **91**, 5203 (2002).
[26]A. Uddin A, A. C. Wei, and T. C. Andersson, Thin Solid Films **483**, 378 (2005).
[27]A. Link, K. Bitzer, W. Limmer, and R. Sauer, J. Appl. Phys. **86**, 6256 (1999).
[28]M. Kuball, S. Rajasingam, A. Sarua, M. J. Uren, T. Martin, B. T. Hughes, K. P. Hilton, and R. S. Balmer, Appl. Phys. Lett. **82**, 124 (2003).
[29]H. Harima, J. Phys.: Condens. Matter **14**, R967 (2002).
[30]L. W. Ji, T. H. Fang, and T. H. Meen, Phys. Letts A **355**, 118 (2006).
[31]A. Link, K. Bitzer, W. Limmer, R. Sauer, C. Kirchner, V. Schwegler, M. Kamp, D. G. Ebling, and K. W. Benz, J. Appl. Phys. **86**, 6256 (1999).
[32]J. M. Hayes, M. Kuball, Y. Shi, and J. H. Edgar, Jpn. J. Appl. Phys. **39**, L710 (2000)
[33]O. N. Ermakov, M. G. Kaplunov, O. N. Efimov, I. K. Yakushchenko, M. Yu. Belov, and M. F. Budyka, Microelectron Eng. **69**, 208 (2003).
[34]E. Kuokstis, R. Gaska, M. S. Shur, J. W. Yang, G. Simin, and M. A. Khan, Appl. Phys. Lett. **80**, 977 (2002).
[35]S. Nakamura, Science **281**, 956 (1998).
[36]Y. Narukawa, Y. Kawakami, M. Funato, S. Fujita, S. Fujita, and S. Nakamura, Appl. Phys. Lett. **70**, 981 (1997).
[37]E. Berkowics, D. Gershoni, G. Bahir, A. C. Abare, S. P. DenBaars, and L. A. Coldren, Phys. Stat. Sol. B **216**, 291(1999).
[38]I.-K. Park, M.-K. Kwon, S.-H. Baek, Y.-W. Ok, T.-Y. Seong, S.-J. Park, Y.-S. Kim, Y.-T. Moon, and D.-J. Kim, Appl. Phys. Lett. **87**, 061906 (2005).
[39]Z. Vaitonis, P. Vitta, and A. Zukauskas, J. Appl. Phys. **103**, 093110 (2008).
[40]J. Hu, L. Yang, L. Kim, and M. W. Shin, Semicond. Sci. Technol. **22**, 1249 (2007).
[41]Y. P. Varshni, Physica **34**, 149 (1967).
[42]C. G. Moe, M. L. Reed, G. A. Garrett, G. D. Metcalfe, T. Alexander, H. Shen, and M. Wraback, IEEE CFP09RPS-CDR 47th Annual International Reliability Physics Symposium, Montreal, 2009, p. 94.
[43]H. Masui, S. Nakamura, and S. P. DenBaars, Appl. Phys. Lett. **96**, 073509 (2010).
[44]T. Sah, R. N. Noyce, and W. Shockley, Proc. IRE **45**, 1228 (1957).
[45]Y. L. Khait, J. Saizman, and R. Beserman, Appl. Phys. Lett. **53**, 2135 (1988).
[46]X. A. Cao, P. M. Sandvik, S. F. LeBoeuf, and S. D. Arthur, Micro. Rel. **43**, 1987 (2003).
[47]A. Uddin, T, A. C. Wei, and T. G. Andersson, Thin Solid Films **483**, 378 (2005).
[48]O. Pursiainen, N. Linder, A. Jaeger, and R. Oberschmid, Appl. Phys. Lett. **79**, 2895 (2001).
[49]S.-L. Chuang, A. Ishibashi, S. Kijima, N. Nakayama, M. Ukita, and S. Taniguchi, IEEE J. Quantum Electron. **33**, 970 (1997).
[50]*Semiconductor Optoelectronics-Physics and Technology*, edited by J. Singh (McGraw-Hill, Singapore, 1995).

Downloaded 08 Nov 2011 to 158.132.161.9. Redistribution subject to AIP license or copyright; see http://jap.aip.org/about/rights_and_permissions